Talanta 118 (2014) 270–276

Contents lists available at ScienceDirect

Talanta

journal homepage: www.elsevier.com/locate/talanta

Gold nanoparticle modified capacitive sensor platform for multiple marker detection

Zeynep Altintas [a], Sreenivasa Saravan Kallempudi [b], Yasar Gurbuz [a,*]

[a] Faculty of Engineering and Natural Science, Sabanci University, Orhanli, Tuzla, Istanbul 34956, Turkey
[b] Sabanci University Nanotechnology Research and Application Centre (SUNUM), Sabanci University, Orhanli, Tuzla, Istanbul 34956, Turkey

ARTICLE INFO

Article history:
Received 24 May 2013
Received in revised form
3 October 2013
Accepted 15 October 2013
Available online 25 October 2013

Keywords:
Capacitive biosensors
Gold nanoparticle
Multiple marker detection
Cancer biomarkers
Cancer detection

ABSTRACT

The detection and quantification of cancer biomarkers in human blood is crucial to diagnose patients in the early stage of a disease. The recent advances in biosensor technology can improve detection by reducing the application time and cost without an invasive approach. In this study, a highly sensitive, novel nanoparticle-modified capacitive sensor was developed for the detection of cancer markers. The current work mainly focused on developing a surface modification protocol for achieving higher sensitivity using Au-NPs. An interdigitated electrode (IDE) transducer was modified using gold nanoparticles (Au-NPs) for signal enhancement, the platform was initially optimized with a small size IL-6 protein and the methodology was then applied for multiple marker detection with the aim of precise disease diagnostics. Carcinoembryonic antigen (CEA) and epidermal growth factor receptor (hEGFR) could be successfully detected in the concentration range of 20–1000 pg mL^{-1} while cancer antigen 15-3 (CA15-3) was detected in the range of 10–200 U mL^{-1}. These results show an increase of sensitivity by five-fold with respect to those not modified, demonstrating a highly sensitive and specific capacitive immunoassay that has a great potential for the use of early diagnosis of cancer disease.

1. Introduction

Capacitive sensors can be divided into two groups as faradaic and non-faradaic sensors depending on the transient current flow. In a faradaic process charges are transferred across an interface whereas transient currents can flow without addition of a redox charge transfer in non-faradaic processes. Therefore, redox species are alternately oxidized and reduced by the transfer of an electron to and from the metal electrode in faradaic capacitive sensors. Due to this, these kind of capacitive sensors require the addition of a redox-active species and DC bias conditions. On the other hand, additional reagent is not required in non-faradaic sensor and this behavior makes them more amenable to point-of-care applications [1]. The principle of the measurement depended on the changes in dielectric properties and charge distribution while antibody-antigen or probe-DNA/RNA complexes occurred on the electrode surface in non-faradaic case. In the event of a conformational change of a surface protein through binding of an analyte, this can be detected by capacitance measurements. The capacitance measurement can be realized through the measurement of the change in the capacitance between two metal conductors in near proximity to one another with the recognition element immobilized on IDEs. The detection principle of the sensor system is based on capacitive coupling of the excitation signal (conductivity and permittivity of medium) produced by IDE electrodes [2]. Thus, the electric field lines always penetrate into the accumulating medium (antigen-antibody complex) regardless of the position of the electrodes (parallel or co-planar). Depending on the geometric configuration of the electrodes, the electric field lines can penetrate deeper with wider electrode configuration [2]. Therefore, the capacitance of the IDE always depends on the geometry of the electrodes that is constant and the dielectric property of the medium. For interdigitated electrodes, the capacitance is defined with the following equation:

$$C = \varepsilon\varepsilon_o \frac{A}{d} \quad (1)$$

where, ε is the dielectric constant of the medium between the plates, ε_o (8.85419 pF/m) is the constant of permittivity of free space, A is the area of the plates and d is the distance between the plates. Immunoassays on the IDE transducer surface generally occur by the deposition of different biochemical layers (SAM, antibodies, Au-NPs and antigens) that increase the probe layer thickness, and thus, all biological samples have an arrangement of electric charge carriers [3]. These charges are displaced by an external electric field and polarized to neutralize the effect of the external electric field. This dielectric response of each type of protein over the frequency spectrum is unique in its characteristic [4]. Therefore, if a change occurs in the dielectric properties in the supplies between the plates, it leads to a change in the capacitance [5].

Interdigitated finger electrodes (IDE) have been used to obtain a larger sensor surface and with some modifications on IDE's they

* Corresponding author. Tel.: +90 216 483 9533; fax: +90 216 483 9550.
E-mail address: yasar@sabanciuniv.edu (Y. Gurbuz).

0039-9140/$ - see front matter © 2013 Elsevier B.V. All rights reserved.
http://dx.doi.org/10.1016/j.talanta.2013.10.030

provide the direct detection of many entities including acetylcoline, toxin, oxygen bubbles, HIV and human IgG antibodies. A complex protein includes hydrophobic and hydrophilic regions, and the protein folds in a soluble media depending on this behavior. While a protein is immobilized on a solid surface and allowed to bind its analyte, a protein–analyte complex is formed. The change in conformation brought on by this interaction leads to an increase in molecular size of a protein–analyte complex. Hence, a local disturbance of the distribution of bound charges will occur at the dielectric interface, and these charges move under strong confinement and their local moment is termed as dipole moment [6]. Thus, increase in size of a protein–analyte complex leads to a relatively large permanent dipole moment which stimulate dielectric polarization on the IDE surface [5]. Therefore, the measured impedance/capacitance of the IDE varies with the relative change of the dielectric properties of the modified surface medium.

In most label-free faradaic-/optical-based biosensor systems, the nanoparticles were utilized to amplify the signal. Here, an electrochemical-based non-faradaic capacitive sensor was employed and developed for multiple cancer marker detection. In order to achieve higher sensitivity for determining very small sized analytes, a new solid-phase surface-modification protocol have been developed. In fact, we demonstrated recently that micro-sized magnetic beads can also be used as a solid-phase support material for determining very small sized analytes [7]. The surface coverage with the large sized magnetic beads and an extra process step of sandwich assay in the developed protocol hinder its further applications. Here, the sensor was modified with gold nanoparticles (Au-NPs) that have unique properties [8–11]. The Au-NPs modified sensor (IDE) surface provides stability for the immobilization of biomolecules that retain their biological activities (probably due to enhanced orientational freedom) which is extremely useful when preparing label-free impedimetric biosensors. Various characteristics of gold nanoparticles, such as their high surface-to-volume ratio, their high surface energy, their ability to decrease the distance between proteins and metal particles, and their ability to act as an electron-conducting pathway between prosthetic groups and the electrode surface, may facilitate electron transfer between redox proteins and the electrode surface [8]. In addition, it is noted that using covalent approach towards the directed self-assembly of gold nanoparticles from solution results in dense monolayer coverage of the particles on the IDE surface. The interaction between the gold nanoparticles and the IDE is mediated by a weak covalent bond. This allows the immobilization of dense networks of gold nanoparticles on IDE surface, which is of interest for use in label-free electrical detection system to achieve higher sensitivity by increasing the density of biological species within the constant sensor area.

Biosensors can be constructed by immobilizing the biomolecules by adsorbing them onto the nanoparticles, by cross-linking them with bi-functional agents such as glutaraldehyde, or by mixing them with the other components of composite electrodes [12]. Moreover, the nanoparticle surface can generate highly-active and large surface area. This enables binding of ultra low target concentrations and increases the density of biological species within the constant sensor area. In this work, the interdigitated capacitive transducer was modified with Au-NPs after SAM formation for signal amplification to detect trace amount of biomarkers in multiple cancer marker detection which has crucial role for precise cancer definition [13–16].

2. Materials and methods

2.1. Materials and reagents

Phosphate buffered saline (PBS) and 2× 4-(2-hydroxyethyl)-1-piperazineethanesulfonic acid (HEPES) buffer were purchased from PAN BIOTECH GmbH, Germany and Fluka, Germany, respectively. Ethanolamine (99%), bovine serum albumin (BSA), human serum, mouse monoclonal antibody to human IL-6, human IL-6 antigen, thiourea, N-(3-dimethylaminopropyl)-N-ethylcarbodiimide hydrochloride (EDC) and N-hydroxysuccinimide (N-hydroxy-2,5-pyrrolidinedione, NHS), sheep monoclonal antibody to human epidermal growth factor receptor (anti-hEGFR), human epidermal growth factor receptor (hEGFR) and human serum were purchased from Sigma-Aldrich (USA). CEA and CA15-3 antigens and their monoclonal antibodies were bought from Fitzgerald (USA). Carboxy encapsulated gold nanoparticles were purchased from NanoComposix (San Diego, CA). Doubly distilled water (dH_2O) was used throughout the experiments.

2.2. Preparation of Au-NP modified sensor platform

IDEs were patterned on silica (SiO_2) surface using image reversal technique. In this process, the metal layers were patterned using the dual tone photoresist AZ5214E. A 2-μm thick AZ5214E photo resist was used to create an inverse pattern of the mask design. Following this step, a very thin titanium (Ti) layer of ~20 nm size was layered to improve the adhesion of gold (Au) on the SiO_2 film by direct current (DC) sputter deposition, and about ~180 nm thick gold layer was deposited. The lift-off process was performed by washing away the sacrificial photoresist (AZ5214 E) in pure acetone. As a result, IDE array containing 24 gold interdigitated fingers were patterned. The dimension of each finger electrode was 800 μm in length, 40 μm in width.

The fabricated sensor chip was washed several times with ethanol and rinsed with sterile dH_2O. The cleaned surface was dried by nitrogen gun. The blank measurements were taken by Network Analyzer prior to any surface/bio-chemical treatment/application on the surface. The sensor surface was then coated with self-assembled monolayer (SAM) by immersing the sensor in 10 mM solution of thiourea for overnight incubation followed by rinsing with ethanol and dH_2O and then dried using nitrogen gun. The formation of SAM layer on the surface was confirmed by Fourier transform infrared spectroscopy (FT-IR). Carboxy encapsulated Au-NPs that have 5-nm size was prepared using the buffer solution in 27 μg mL^{-1} concentration [17]. After 8 h of incubation with Au-NPs onto the IDE, the modified surface was activated using 50 mM EDC and NHS and incubated for 3 h. The sensor platform was then washed with PBS and dH_2O. The impedimetric response of Au-NP modified IDE was measured using a Network Analyzer.

2.3. Antibody immobilization

Prior to the multiple marker detection assays for cancer biomarkers, the Au-NP modified sensor platform was optimized using IL-6-anti-IL-6 antigen-antibody pair as model analyte. For this, the Au-NP modified IDE surfaces of capacitors were immobilized by incubating 2.5 μL of 25 μg mL^{-1} IL-6 antibody in PBS buffer for 1 h. The sensor wafer was then washed with PBS and dried prior to the blocking step with ethanolamine. The non-reacted groups on the sensor surface were blocked by adding 5 μL of 100 mM ethanolamine on each IDE and incubated for 1 h. The sensor was then rinsed with PBS and sterile dH_2O, and dried with nitrogen gun prior to the measurements for antibody immobilization using a Network Analyzer. The analyzer was calibrated and triplicate measurements were then taken for each electrode for error analysis. The protocol developed for enhanced sensitivity was shown as schematic in Fig. 1a.

2.4. Capacitance measurements

To measure dielectric parameters (impedance/capacitance), a Karl-Suss (PM-5) RF Probe Station and an Agilent-8720ES S-parameter

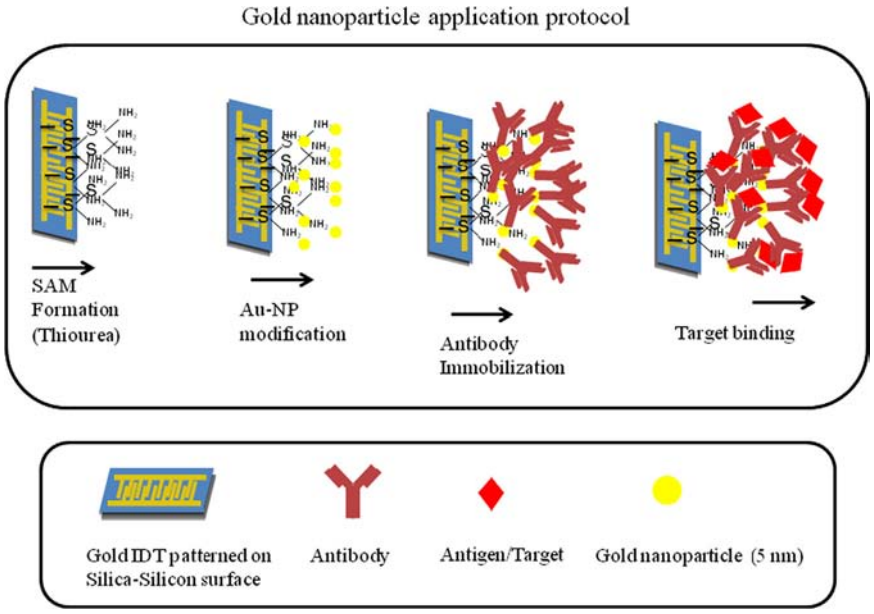

Fig. 1. The principle of the applied bioassay using the Au-NP modification (i) thiolization of GID surface using thiourea, (ii) covalent binding of gold nanoparticles, (iii) blocking of IDE surface (after antibody immobilization) with ethanolamine, and (iv) direct assay formation with specific antigens.

network analyzer were used. The scanned frequency range was between 50 MHz and 1 GHz. The network analyzer was calibrated using the short-open-load-through (SOLT) method (which is a calibration method where dielectric parameters were measured on a reference plane) and S11-parameter data of the capacitive sensor were measured. Dielectric parameters (impedance/capacitance) were measured at four different stages. First, dielectric parameters were measured using (a) blank measurements for checking the working condition of the IDE's to design the experiment, (b) after Au-NP modification, (c) after antibody immobilization and (d) after antigen/target binding on the IDE immobilized with antibody. All measurements were performed in triplicate for deviation analysis. Further, for analysis, the Matlab tool was used to calculate capacitance from the measured S11 parameter values. Changes in capacitance at an effective frequency were compared (signal from blank, control and after target capturing).

2.5. Protein detection

A series of IL-6 concentrations (0.02–10 ng mL^{-1}) were prepared in 1 × PBS buffer and the same buffer was used as a blank control. Each concentration of the biomarker was tested on three independent IDE capacitors for error analysis. The IL-6 samples prepared in the buffer were incubated for 2 h for the antigen detection step and the sensor was then carefully rinsed with PBS followed by dH_2O to remove traces of salts on the sensor surface. The sensor was quickly dried with nitrogen gas and each IDE capacitor was measured for the detection of IL-6 marker. The specificity of the interaction between the target antibody (anti-IL6) and antigen (IL-6) was checked by applying 10 ng mL^{-1} of BSA protein on the anti-IL6 immobilized electrodes (IDEs) instead of the target protein marker. The average values of the relative change in capacitance were plotted and the standard deviations of the triplicate experiments were shown as error bars.

2.6. Multiple marker assay

The Au-NP modified capacitors were immobilized by incubating 2.5 μL of 25 μg mL^{-1} anti-CEA, anti-hEGFR and anti-CA15-3 antibodies in PBS buffer for 1 h. The sensor wafer was then washed with PBS and dried prior to the blocking step with ethanolamine. The non-reacted groups on the sensor surface were blocked by adding 5 μL of 100 mM ethanolamine on each IDE and incubated for 1 h. The sensors was then rinsed with PBS and sterile dH_2O, and dried with nitrogen gun prior to the measurements for antibody immobilization using a Network Analyzer. The analyzer was calibrated and triplicate measurements were then taken for each IDE electrode for error analysis.

A series of antigen concentrations in the range of 0–1 ng mL^{-1} and 0–200 U mL^{-1} (in case of CA 15-3 protein) were initially prepared on ice. The capacitors were then incubated for 2 h with different antigen concentrations in 2.5 μL volume for each biomarker. The capacitive measurements were taken before and after the antigen treatment. Capacitance change was calculated from the measurements of the sample capacitance and three individual electrodes were used for each antigen concentration to understand the repeatability and reliability of the assays. Capacitance change was calculated from the data measurements in the effective frequency range of 500–1000 MHz for plotting. Negative control assays were also performed using the buffer solution and BSA protein to check the specificity of the assays. The deduced capacitance after antigen binding was normalized with the values obtained from the respective antibody immobilization and the results were analyzed as the normalized capacitance change ($|\Delta C|$).

$$\%|\Delta C| = \frac{C - C_o}{C_o} \times 100 \quad (2)$$

where C and C_o represent the capacitance after target binding and protein immobilization. Average values of response obtained from triplicate experiments were plotted and the standard deviations were calculated that were shown as errors.

3. Results and discussion

3.1. Detection analysis

An IDE operates in a way that is very similar to a conventional parallel plate capacitor where dielectric properties give information

such as conductivity and permittivity of the medium. The detection principle of conductivity and permittivity of medium is based on capacitive coupling of the excitation signal produced by IDE electrodes [2]. Thus, the electric field lines always penetrate into the medium regardless of the position of the electrodes (parallel or co-planar). Depending on the geometric configuration of the electrodes, the electric field lines can penetrate deeper with wider electrode configuration. Therefore, as mentioned in the introduction, the capacitance of the IDE changes with the dielectric property of the surface medium. While developing immunoassay on the IDE surface, different biochemical layers are coated which increases the probe layer thickness and all biological samples have an arrangement of electric charge carriers. These charges are displaced by an external electric field and polarized to neutralize the effect of the external electric field. This dielectric response of each protein over the frequency spectrum is unique characteristic for each of its kind.

The dielectric response of any material is represented in terms of its complex dielectric permittivity ε^* and it is given as

$$\varepsilon^* = \varepsilon' - j\varepsilon'' \tag{3}$$

where the real part of permittivity ε' is called dielectric constant and is a measure of energy stored from an external electric field in a material. The imaginary part of permittivity ε'' is called the loss factor and is a measure of the energy loss to an external electric field. The loss factor is actually expressed as a function of both dielectric loss and conductivity and it is given as

$$\varepsilon^* = \varepsilon' - j\left[\varepsilon''_d + \frac{\sigma}{\omega}\right] \tag{4}$$

where, ε''_d is dielectric loss and σ is conductivity. Depending on their relaxation frequency $\sigma/\omega\varepsilon$, a material falls into two categories: conductive material or dielectric material. In general, when $\sigma/\omega\varepsilon \gg 1$, the material is considered as a good conductor or lossy material. Similarly, the material is considered dielectrics or low-loss material if $\sigma/\omega\varepsilon \ll 1$. Therefore, the intrinsic nature of the biochemical species would affect the imaginary part of dielectric permittivity and hence the dielectric property of the coated medium changes. However, the structure and nature of most protein/biological molecules are not defined to the extent and direct measurements for complex dielectric permittivity are hard to achieve. Alternatively, the relationship between ε' and ε'' with frequency ω as the independent parameter can be estimated using Cole–Cole model [5]. It should be noted that even when the conductivity of a material is zero, its complex dielectric permittivity may have a non-zero imaginary part. The non-zero imaginary part is responsible for the energy dissipation process due to dipole re-orientation and translational motion of charge carriers.

3.2. Determination of IL-6 antigen

A Network Analyzer was employed to record the S11 parameters generated due to the SAM formation, Au-NP application and the detection of IL-6 antigen using IL-6 antibody on each IDE capacitor. For the analysis, the capacitance was deduced from the S11 parameters. After Au-NP modification, 25 μg mL^{-1} was immobilized to the sensor surface for the detection of IL-6 antigen. Different concentrations of IL-6 antigen (0.02–10 ng mL^{-1}) in a final 2.5 μL volume were incubated on each IDE sensor surface in triplicates and PBS buffer was used as a negative control. In labeled/label-free biosensor systems, the optimal concentration of antibody utilized for the immobilization changes between 20 and 50 μg mL^{-1} [18]. Therefore, a preliminary test was also performed prior to this study and a 25 μg mL^{-1} antibody concentration was chosen. The investigated antigen concentration was selected between 0.02 ng mL^{-1} and 10 ng mL^{-1} since we could detect 0.1–10 ng mL^{-1} concentration of IL-6 using standard label-free assay methodology in our previous works [19]. The Au-NP modified sensor platform was initially tested using IL-6 in the selected concentration range and the sensitivity level was then increased with lower concentrations according to the results obtained here.

The specificity of the sensor to IL-6 was derived from the specific binding between the anti-IL6 and IL-6 antigen as there was no binding with BSA protein. The sensor platform was scanned in the frequency range of 50 MHz–1 GHz and inter-assay analysis was performed with three independent experiments. The deduced capacitance after antigen binding was subtracted from the values obtained for only antibody immobilization and the results were analyzed as the normalized capacitance change (% $|\Delta C|$). The normalized capacitance was calculated according to Eq. (2). A clear difference and the sensitivity in response to IL-6 antigen were evident under the applied frequency. For the frequency range analyzed, the antigen was clearly detected in the concentration range of 0.02–10 ng mL^{-1}.

To determine the optimal frequency range of bioassay with Au-NPs, six frequency points between 600 and 1000 MHz were selected and validated and the capacitive response showed saturation after 800 MHz frequency point as seen in Fig. 2. It was understood that frequency range was fitted with our normal scanned frequency range (50 MHz–1 GHz) for biological assays in the platform since the best results were usually obtained between the range of 600–850 MHz (Fig. 3).

We previously investigated IL-6 marker using standard assay methodology (without any solid-phase surface-modification, label-free) in the concentration range of 0.1–10 ng mL^{-1} and the obtained signal was much lower than the Au-NP modified sensor surfaces [19]. The 10 ng mL^{-1} concentration of IL-6 gave a normalized capacitance value of ~0.35 and ~2 response with standard and modified sensor platforms, respectively. Moreover, 0.02 ng mL^{-1} IL-6 could be detected through Au-NP modified capacitors with 1.85 pF capacitance change whereas the detection limit of the standard assay for IL-6 was 0.1 ng mL^{-1}. The detailed comparison can be shown in Table 1.

3.3. Multiple marker assay for precise disease diagnostics

In this study, multiple markers of lung cancer were investigated using Au-NP modified capacitive sensor platform for the first time. With this aim, three target protein markers (CEA, hEGFR and CA15-3) were selected due to their presence at elevated levels in human blood for the cancer cases.

Au-NP modification was carried out after SAM formation with thiourea for signal enhancement via the increase of surface for the

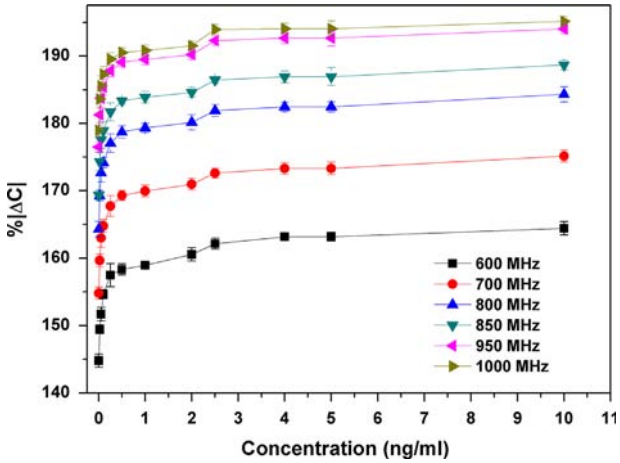

Fig. 2. Capacitive responses of SAM-coated and Au-NP modified sensor surfaces for five electrodes (a). All investigated concentration range of IL-6 at selected 6 frequency points to determine the optimal frequency range for the bioassay (b).

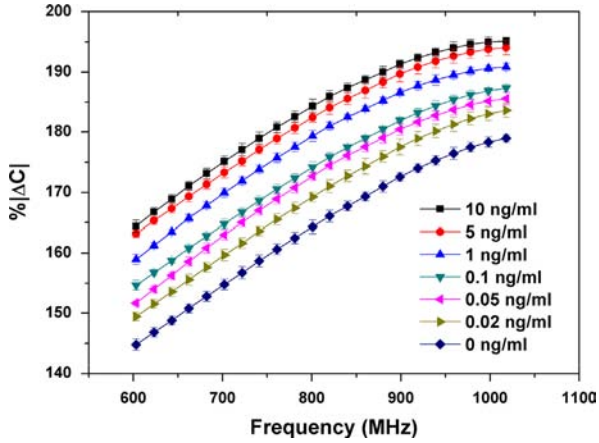

Fig. 3. Capacitive detection of IL-6 marker with standard errors in the frequency range of 600–1100 MHz.

Table 1
Comparison of IL-6 detection for standard (label-free methodology) and Au-NP modified capacitive sensor platforms.

	Standard assay (label-free methodology)	Au-NP modification
Concentration range (ng mL^{-1})	0.1–10	0.02–10
% |ΔC| for 10 ng mL^{-1} IL-6	~35	~195
% |ΔC| for lowest IL-6 concentrations	~32	~185
Detection limit (ng mL^{-1})	0.1	0.02
Signal increase (fold)	1	~6

biological molecules. After the modification of the sensor surface with Au-NP during 8 h incubation, antibody immobilization was performed using three different target antibodies. Antigen binding step of the bioassay was then applied in the concentration range of 5 pg mL^{-1}–1 ng mL^{-1} for CEA and hEGFR while 1–100 U mL^{-1} for CA15-3. The capacitance change of Au-NP modified sensors using CEA, hEGFR and CA15-3 cancer markers were normalized and correlated to the protein complex formation. The specificity of the assays is also verified using a BSA protein (10 ng mL^{-1}) and normalized response was observed between the response levels of lowest concentration of the antigen and the controls. PBS buffer (0 pg mL^{-1} CEA, EGFR or CA15-3) was also tested as negative control on the sensor surfaces immobilized with antibody (anti-CEA, anti-hEGFR and anti-CA15-3) to measure the baseline response of the solution used for the preparation of the samples. The capacitive responses of the sensors were plotted in the optimal frequency range for protein markers (Fig. 4).

The results of CA15-3 detection were plotted separately due to the difference between concentration types. The normal range of CA15-3 marker in human blood is 50 U mL^{-1} [20] and the increased level of the marker plays a role as cancer indicator. The marker has not been tested with sensor technologies using nanoparticle surface-modification methodologies whereas ELISA tests have been conducted for clinical analysis and disease diagnostics. Moreover, this marker has been investigated as units per milliliter instead of molar concentration due to its enzymatic behavior and the detection limits of commercially available ELISA kits change between 5 and 10 U mL^{-1}. The concentration of samples for CA15-3 marker was prepared according to the threshold level of the marker in human blood and ELISA tests and the concentration range of 1–100 U mL^{-1} was successfully detected.

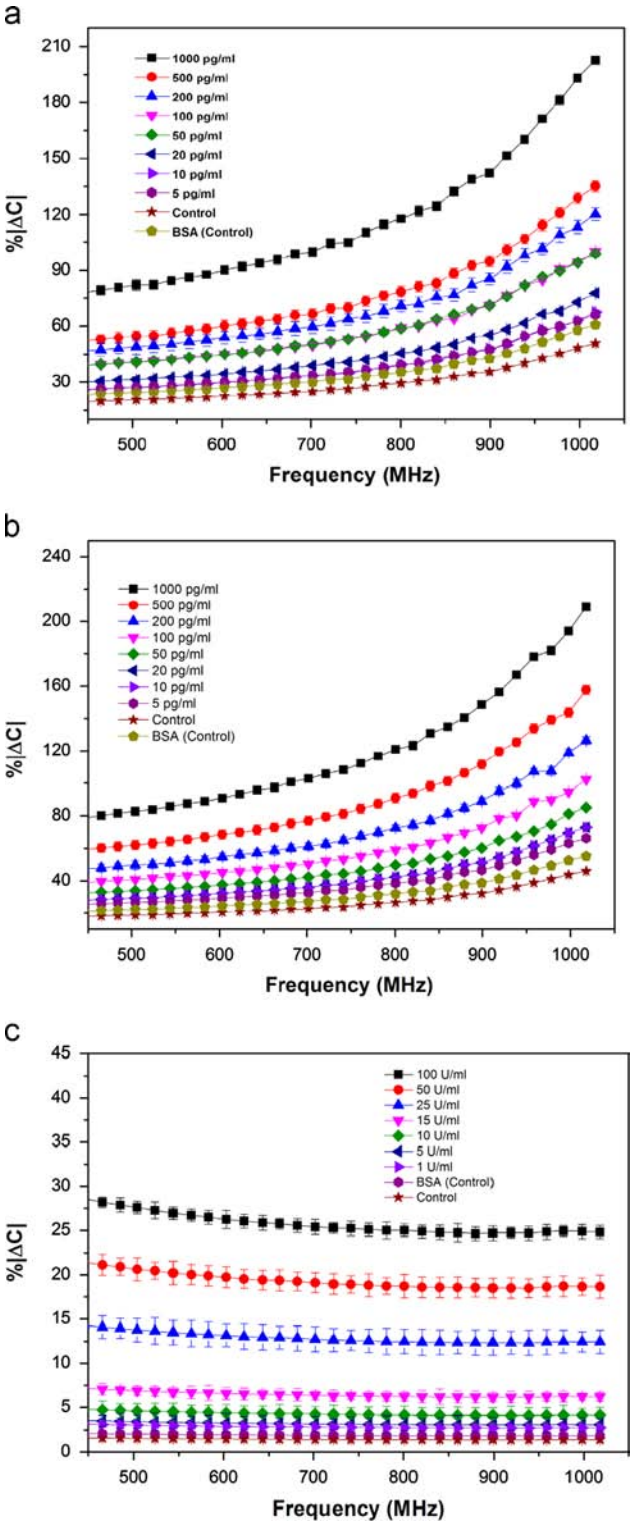

Fig. 4. Capacitive detection of CEA, hEGFR and CA15-3 cancer markers in buffer solution with Au-NP modified capacitive sensor in the frequency range of 450–1000 MHz. CEA and hEGFR detection in the concentration range of 5–1000 pg mL^{-1} (a, b). CA15-3 marker detection in the concentration range from 1–100 U mL^{-1} (c).

3.4. Multiple marker detection in human serum

There is a significant difference for the detection limit of markers when buffer or human serum is used as the assay media. The detection limit is high when the real serum samples are used due to the lower signal to noise ratio resulting from high

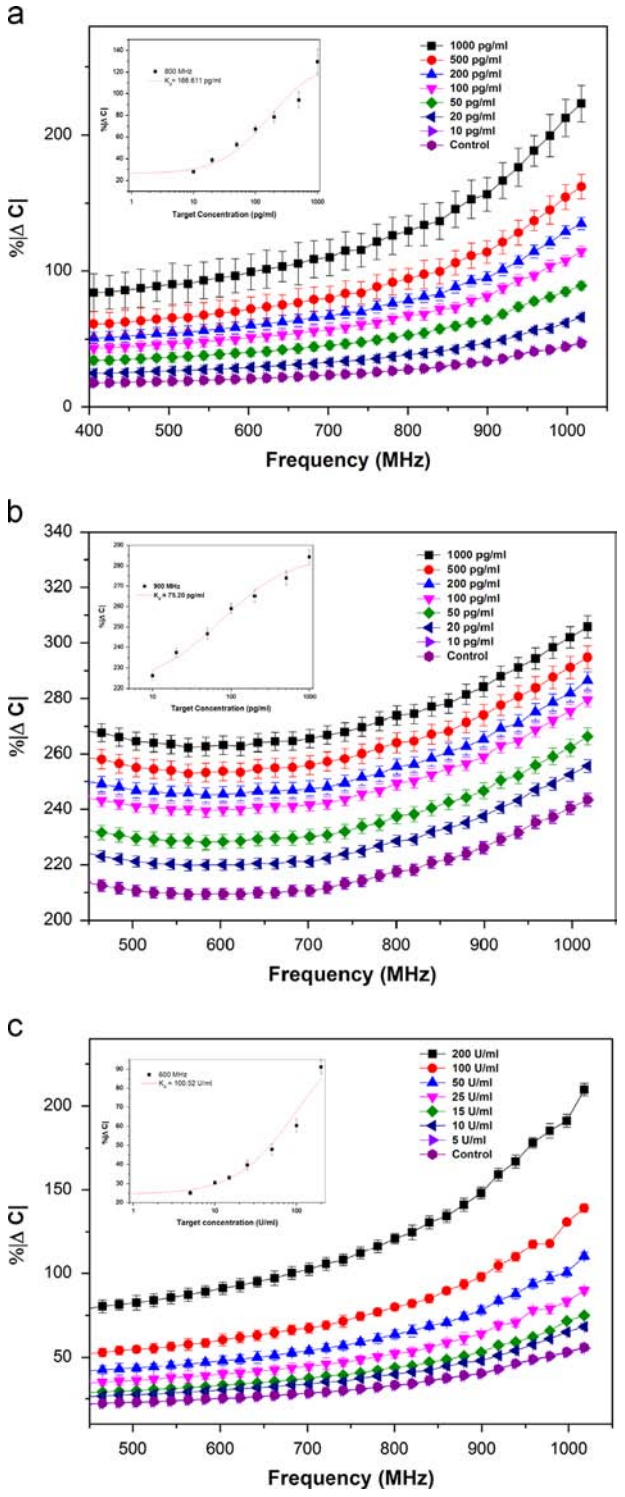

Fig. 5. Relative change in capacitance while testing CEA, hEGFR and CA15-3 cancer markers spiked with human serum using Au-NP modified capacitive sensor in the frequency range of 450–1000 MHz. CEA and hEGFR detection in the concentration range of 20–1000 pg mL^{-1} (a, b). CA15-3 marker detection in the concentration range from 10–200 U mL^{-1} (c).

non-specific binding of serum proteins on the sensor surface. Due to these facts, the real serum samples were also tested for CEA, EGFR and CA15-3 markers in the current study. The same experimental strategy was performed and the investigated concentration ranges for the markers were selected as 5–1000 pg mL^{-1} (for CEA and EGFR) and 5–200 U mL^{-1} (CA15-3). 2.5 μL of serum (as 0 pg mL^{-1} concentration for each marker) was used as the control. The detection limits of the markers in real serum were found as 20 pg mL^{-1} for CEA and EGFR while it was 5 pg mL^{-1} when the buffer solution was used as the assay media (Fig. 5a and b). The detection limit for CA15-3 marker in real serum samples was calculated as 10 U mL^{-1} while it was 1 U mL^{-1} for buffer samples (Fig. 5c). Although the minimum concentration of the target detected was increased for each marker when the real serum samples were tested, the achieved limits have been still much lower than the disease threshold levels of the markers (5 ng mL^{-1}, 64 ng mL^{-1}, and 50 U mL^{-1} for CEA, hEGFR and CA15-3, respectively) [20–22].

Further, non-linear regression fit analysis was performed in the dynamic detection range of 0–1000 pg mL^{-1} for CEA and hEGFR, and 0–100 U mL^{-1} for CA15-3 proteins to determine the binding affinity between target antibody-antigen pair on the Au-NP modified sensor platform and dissociation constants were extracted. According to the Langmuir adsorption isotherm, the smaller the dissociation constant value the stronger the binding affinity between the antibody–antigen pair can be observed at specific frequency points, respectively, as shown in the insets of Fig. 5a–c [23]. The results of CEA and EGFR detection according to the antigen concentration were found very similar while the obtained signal was quite different when compared with CA15-3 protein. The similarity of the results for CEA and EGFR may depend on the molecular weight of the markers that are very close to each other and the same concentration level of the prepared samples. The results of CA15-3 tests showed difference due to the concentration type (units per milliliter instead of picograms per milliliter) when compared with the other markers and the sample concentrations of CA15-3 were in trace amount in this study. The marker could be successfully detected at 10 U mL^{-1} concentration using Au-NP modified sensor platform which is much lower than the threshold level and ELISA kits.

We observed that the sensor response did not reach to a saturation level above a concentration of 1 ng mL^{-1} (hEGFR and CEA) and 200 U mL^{-1} (in sights of Fig. 5). Therefore, for 25 μg mL^{-1} antibody concentration there are available protein-binding sites. This could be due to the high surface active area provided by the Au-NP's. With the employed label-free methodology, there exists limited work performed for the quantification of cancer markers. From our laboratory, we reported a detection limit of 3 ng mL^{-1} in serum for hEGFR [19]. In this work, for 25 μg mL^{-1} of anti-hEGFR on a specified area, we achieved a detection limit of 20 pg mL^{-1} in serum.

The current work mainly focused on developing a surface modification protocol for achieving higher sensitivity using nanoparticles. The surface distribution of nanoparticles is controllable and uniform when compared to our previous work [7]. Moreover, we achieved the same sensitivity without sandwich assay. The successful achievement of this study with Au-NP modified biosensor may be due to (a) ability of Au-NPs to provide a more stable surface for antibody immobilization that retain their biological activities, (b) capture of more antigen due to more antibody on Au-NPs, (c) enhancement of orientational freedom for antigen binding on Au-NP modified sensor, (d) high surface to volume ratio and surface energy of Au-NPs, and (e) ability of Au-NPs to decrease the distance between proteins and metal particles [8,24].

4. Conclusion

Most biosensors systems often lose their analytical efficiencies while working with serum-based biological samples. Therefore, achieving higher sensitivity and selectivity, regeneration of sensor surface and sensor life-time are the major issues in the development of such serum-spiked electrode-based biosensor systems.

The current work mainly focused on developing a surface modification protocol for achieving higher sensitivity using gold nanoparticles. In this study, a gold nanoparticle-modified capacitive sensor was developed and optimized using anti-IL6-IL-6 protein pair. The IL-6 was investigated in the concentration range of 0.02–10 ng mL^{-1} for the frequency range of 450–1000 MHz. The optimized methodology in the same frequency range was then implemented to the multiple marker detection research to quantify lung cancer biomarkers. Artificial human serum spiked with CEA, hEGR and CA15-3, lung cancer biomarkers, were successfully detected in the concentration range of 20 pg mL^{-1}–1 ng mL^{-1} and 10–200 U mL^{-1}, respectively. The signal enhancement approach using Au-NP modified sensor platform has provided an alternative detection tool for precise and early diagnosis of the cancer that is the most crucial point in treatment. Moreover, nanoparticle modification indicated an effective method for the quantification of small size biological molecules such as IL-6 (24 kD) which has also low threshold levels in disease conditions. The results show the promising usage of Au-NPs in our capacitive platform and the useful alternative diagnostic approach for disease markers.

Acknowledgment

This research was supported by TUBITAK under the Project code 110E287.

References

[1] J.S. Daniels, N. Pourmand, Electroanalysis 19 (2007) 1239–1257.
[2] A.V. Mamishev, K. Sundara-Rajan, F. Yang, Y. Du, M. Zahn, Proc. IEEE 92 (2004) 808–845.
[3] S. Linse, P. Brodin, C. Johansson, E. Thulin, T. Grundström, S. Forsén, Nature 335 (1988) 651–652.
[4] C. Gabriel, S. Gabriel, E. Corthout, Phys. Med. Biol. 41 (1996) 2231.
[5] S.S. Kallempudi, Y. Gurbuz, Sensors Actuators B: Chem. 160 (2011) 891–898.
[6] S. Grimnes, Ø. Martinsen, Bioimpedance and Bioelectricity Basics, Academic press, London, 2008.
[7] Z. Altintas, S.S. Kallempudi, U. Sezerman, Y. Gurbuz, Sensors Actuators B: Chem. 174 (2012) 187–194.
[8] E. Katz, I. Willner, J. Wang, Electroanalysis 16 (2004) 19–44.
[9] B. Shlyahovsky, E. Katz, Y. Xiao, V. Pavlov, I. Willner, Small 1 (2005) 213–216.
[10] D. Shitrit, B. Zingerman, A.B.G. Shitrit, D. Shlomi, M.R. Kramer, The Oncologist 10 (2005) 501–507.
[11] B. Shlyahovsky, E. Katz, Y. Xiao, V. Pavlov, I. Willner, Small 1 (2005) 213–216.
[12] P. Yanez-Sedeno, J. Pingarron, Anal. Bioanal. Chem. 382 (2005) 884–886.
[13] R. Etzioni, N. Urban, S. Ramsey, M. McIntosh, S. Schwartz, B. Reid, et al., Nat. Rev. Cancer 3 (2003) 243–252.
[14] R. Fan, O. Vermesh, A. Srivastava, B.K.H. Yen, L. Qin, H. Ahmad, et al., Nat. Biotechnol. 26 (2008) 1373–1378.
[15] S.L. Liang, D.W. Chan, Clin. Chim. Acta 381 (2007) 93–97.
[16] G. Zheng, F. Patolsky, Y. Cui, W.U. Wang, C.M. Lieber, Nat. Biotechnol. 23 (2005) 1294–1301.
[17] S. Loyprasert, P. Thavarungkul, P. Asawatreratanakul, B. Wongkittisuksa, C. Limsakul, P. Kanatharana, Biosensors Bioelectron. 24 (2008) 78–86.
[18] M.A. Cooper, Label-free biosensors, Techniques and Applications, Cambridge University Press, New York, 2009.
[19] S.S. Kallempudi, Z. Altintas, J.H. Niazi, Y. Gurbuz, Sensors Actuators B: Chem. 163 (2012) 194–201.
[20] Y. Kimura, T. Fujii, K. Hamamoto, N. Miyagawa, M. Kataoka, A. Iio, Br. J. Cancer 62 (1990) 676.
[21] Z. Altintas, Y. Uludag, Y. Gurbuz, I.E. Tothill, Talanta 86 (2011) 377–383.
[22] W.P. Carney, Expert Rev. Mol. Diagnostics 7 (2007) 309–319.
[23] R. Fowler, A Statistical Derivation of Langmuir's Adsorption Isotherm, Cambridge University Press, New York, (1935) 260–264.
[24] S. Loyprasert, M. Hedström, P. Thavarungkul, P. Kanatharana, B. Mattiasson, Biosensors Bioelectron. 25 (2010) 1977–1983.